Am J Transl Res 2022;14(7):4591-4605
www.ajtr.org /ISSN:1943-8141/AJTR0142715

Original Article

Arsenic exposure increases susceptibility to *Ptpn11*-induced malignancy in mouse embryonic fibroblasts through mitochondrial hypermetabolism

Fan Yang, Zhenya Tan, Yuanjuan Dai, Xingxing Wang, Zhen Huang, Chen Kan, Siying Wang

Department of Pathophysiology, School of Basic Medical Sciences, Anhui Medical University, Hefei, Anhui, China

Received March 6, 2022; Accepted May 5, 2022; Epub July 15, 2022; Published July 30, 2022

Abstract: Objective: To explore the synergistic effect and metabolic mechanism of chronic arsenic exposure and *PTPN11* gain-of-function mutation on tumorigenesis. Methods: Arsenic-transformed *Ptpn11*$^{+/+}$ (WT-As) and *Ptpn11*$^{D61G/+}$-mutant (D61G-As) mouse embryonic fibroblasts (MEFs) were established by chronic treatment of low-dose arsenic. We used cell counting, plate colony and soft agar colony formation, and a nude mouse xenograft model to detect malignant transformation and tumorigenesis *in vitro* and *in vivo*. To detect mitochondrial oxidative phosphorylation (OXPHOS), we used Seahorse real-time cell metabolic analysis as well as adenosine triphosphate (ATP) and ROS production assays. Lastly, we examined mTOR signaling pathway changes by western blotting. Results: Low-dose arsenic exposure promoted WT MEFs proliferation and exacerbated malignancy driven by *Ptpn11*$^{D61G/+}$ mutation. Additionally, *Ptpn11*$^{D61G/+}$-mutant MEFs exhibited increased mitochondrial metabolism and low-dose arsenic amplified this malignant metabolic activity. Mechanistically, the mTOR signaling pathway was activated in *Ptpn11*$^{D61G/+}$-mutant MEFs and was further phosphorylated in arsenic-treated MEFs expressing *Ptpn11*$^{D61G/+}$. Critically, tumorigenesis induced by the synergistic effect of low-dose arsenic and *Ptpn11*$^{D61G/+}$ mutation was prevented by mTOR pathway inhibition via rapamycin. Conclusion: This study found that metabolic reprogramming, particularly mitochondrial hyperactivation, is a core mechanism underlying tumorigenesis induced by the synergistic effect of *Ptpn11*$^{D61G/+}$ mutation and arsenic exposure. Furthermore, these findings suggested mTOR is a therapeutic target for *Ptpn11*-associated cancers.

Keywords: Arsenic, PTPN11, mitochondrial hypermetabolism, mTOR

Introduction

Genetic and epigenetic alterations, including mutations in oncogenes or tumor suppressor genes, are well-known factors that promote tumorigenesis [1, 2]. In-depth studies on the carcinogenic effects of environmental factors confirmed that long-term exposure to heavy metal pollutants contributes to the development of skin, lung, and bladder cancers [3, 4]. The high incidence and early onset of tumors is likely due to a combination of multiple factors [5, 6]. However, whether there is a synergistic effect between different genetic factors and environmental carcinogens, and the underlying mechanism remains unknown.

The non-receptor protein-tyrosine phosphatase SHP-2, which is encoded by the *PTPN11* gene, plays an important role in regulating proliferation, differentiation, and metastasis [7, 8]. SHP-2 consists of two Src homology 2 (SH2) domains at the N-terminal, a tyrosine phosphorylation catalytic domain in the middle of the protein, and two tyrosine phosphorylation sites at the C-terminal site [9]. SHP-2 exists in a dynamic equilibrium between closed (inactive) and open (active) states. Crystal structure analysis revealed that, without interference, SHP-2 is self-inhibited and its N-SH2 domain binds to the catalytic cleft of the PTP. N-SH2/PTP interface (*e.g.*, E76K/D61Y) gain-of-function (GOF) mutations can lead to conformational activation of the protein [10]. In addition, SHP2 can be activated through the exposure of catalytic gaping of the substrate when the phosphotyrosine peptide binds to the opposite side of the N-SH2 domain [11]. SHP-2 GOF mutations have

been associated with the development and progression of various tumor types, such as Noonan syndrome (NS), juvenile myelomonocytic leukemia (JMML), and other sporadic solid tumors [12, 13]. Of SHP-2 GOF mutations, the D61G mutation, known as a NS-associated mutation, has been found in NS and leukemia in humans and animal models [14, 15]. Although one case of gastric cancer harboring the SHP-2 D61G mutation was reported in the Catalogue of Somatic Mutations In Cancer (COSMIC) database, this mutation has not been reported in solid tumors. Current studies have focused on the role of this mutation in promoting glioma [16] and breast cancer [17] progression by introducing this mutation *in vitro*. Although SHP-2 activating mutations increase genomic instability and cancer susceptibility due to exposure to external factors, such as cytokines or radiation stimulation [14, 18], it is unclear whether this activating mutation also increases susceptibility to other carcinogenic factors. Even so, the underlying mechanism remains to be determined.

Arsenic is an environmental pollutant that is widely distributed in nature in organic and inorganic forms. Inorganic arsenic is a human carcinogen according to the International Cancer Research Center (IARC). Chronic exposure to small amounts of inorganic arsenic occurs through ingestion of contaminated water or food, use of contaminated water to irrigate crops, and tobacco smoke [20]. Although skin damage is the most obvious and common consequence of chronic arsenic exposure, previous studies demonstrated that chronic arsenic exposure is also associated with the development of many chronic diseases, such as diseases of the nervous system, respiratory system, cardio-cerebrovascular system, and cancer of many tissues and organs, including the lung, skin, bladder, prostate, kidney, and liver [21, 22].

Arsenic carcinogenesis is due to several molecular mechanisms related to DNA damage, including DNA oxidative damage and DNA repair impairment [23]. Additionally, studies have shown low arsenic exposure can enhance the genotoxicity of other agents that cause DNA damage. For example, Chen et al. revealed a significant dose-response relationship between arsenic exposure and lung cancer risk in cigarette smokers [24]. Co-exposure to arsenic and benzo (a) pyrene, which is a polycyclic aromatic hydrocarbon causing DNA lesions, leads to a synergistic effect that causes epigenetic dysregulation and increases lung tumorigenesis [25]. Recent studies have highlighted the involvement of metabolic dysfunctions in the development of arsenic-related tumors [26, 27]. However, the mechanism by which arsenic exposure synergizes with gene mutations to promote carcinogenesis is still unclear.

Tumors energy metabolism reprogramming refers to alterations of tumor cell energy supply in different stages of tumor progression to meet the malignant cellular needs of rapid proliferation, metastasis, invasion, and so on [28, 29]. Such abnormal energy metabolism includes enhanced uptake and utilization of substrates, preferences for different metabolic substrates, such as glucose, amino acids, or fatty acids, and changes in metabolic patterns [30, 31]. Mitochondria, the main organelle specialized for aerobic metabolism, have long been implicated in tumor development and progression [32]. The classic Warburg effect also suggests irreversible mitochondrial damage may be the prerequisite of tumor cell aerobic glycolysis [33]. However, further tumor cell metabolism research has challenged this hypothesis. For example, mitochondrial aerobic metabolism was shown to be the dominant energy source of tumor cells in various cancers, including some leukemias, lymphoma, pancreatic ductal adenocarcinoma, high oxidation metabolic melanoma, and endometrial cancer [34, 35]. In addition to glucose metabolism, lipids or amino acids can become the main energy source for some tumor cells [31, 36]. Even metabolic intermediates of tumor metabolism can reenter the tricarboxylic acid cycle to supplement the deficiency of tumor metabolites. In addition to tumor cell-intrinsic metabolic changes, cells in the tumor microenvironment, such as tumor-associated macrophages, adipocytes, and fibroblasts, also support tumor cell growth through metabolic regulation [28, 38]. These results indicate that tumor metabolic reprogramming is highly dynamic and heterogeneous. Moreover, a tumor cell's energy metabolism properties and preferences evolve during cancer progression in different human tumors.

Studies have demonstrated that *Ptpn11*$^{D61G/+}$ activating mutations enhance ROS production and drive the development of myeloprolifera-

tive diseases and malignant leukemia in mice [14], but the role of these mutations in solid tumors is unclear. Because arsenic exposure in the natural environment is a long-term process that often takes a number of years to cause carcinogenesis, we used *Ptpn11*$^{D61G/+}$ mutated mouse embryonic fibroblasts (MEFs) to establish a cellular model and investigated whether SHP-2 activation mutations synergized with chronic arsenic exposure to drive tumorigenesis. The findings of our research reveal a novel mechanism by which *Ptpn11*$^{D61G/+}$-mutant cells are more sensitive to chronic arsenic exposure, which leading to malignant transformation. Moreover, our results provide a foundation to develop strategies that can prevent or reduce the risk of cancer resulting from arsenic exposure and *Ptpn11*$^{D61G/+}$ mutations.

Materials and methods

Cell culture and reagents

Mouse embryonic fibroblasts (MEFs) were obtained from *Ptpn11*$^{+/+}$ and *Ptpn11*$^{D61G/+}$ mice within 13.5 days using the standard primary MEFs technique and immortalized by SV40 T antigen. MEFs were maintained in Dulbecco's Modified Eagle's Medium (DMEM) supplemented with 10% fetal bovine serum (Life Technologies/Gibco), 100 U/mL penicillin, and 100 μg/mL streptomycin (Invitrogen, Carlsbad, CA). For chronic arsenic treatment, 1×10^5 cells were seeded into 6-cm dishes and were treated with 2 μM As_2O_3 (Sigma) for 48 h when the cells were completely adherent. This process was continued for approximately 3 months.

Soft agar colony formation assay

A total of 2×10^3 arsenic-treated MEFs and control MEFs of the same passage number were resuspended in 1 mL of top layer of agarose media (0.7% agarose). And were then plated on top of the bottom layer (1.2% agarose). To investigate the effect of rapamycin on arsenic-transformed cells, inhibitors were added to the top layer of agarose and culture media. Soft agar colonies were photographed and counted after 2 weeks of incubation under normal conditions.

Nude mouse xenograft tumorigenesis assay

Arsenic-transformed MEFs (2×10^6/0.2 mL) were injected subcutaneously with Matrigel in a 1:1 ratio into the right flank of BALB/C nude mice (5-6 weeks old). Subsequent tumors were grown to a volume of approximately 80 to 200 mm^3. The tumor volume (mm^3) was calculated based on the formula: $V=(l\times w^2)/2$, l and w refers to the larger and smaller widths of the tumor. The mice were sacrificed after a 5-week observation period. The tumors were harvested, weighed, and either snap frozen, stored at -80°C, or processed for paraffin embedding. All breeding and animal experiments were performed in accordance with the guidelines of the university laboratory and with approval from the Animal Experimentation Ethics Committee of Anhui Medical University (No. 20170529).

Western blotting assay

Western blotting was performed as described previously [40]. Briefly, cell precipitation was washed with ice-cold PBS. Cell extracts were obtained using ice-cold lysis buffer supplemented with 0.5% protease inhibitor (Roche, Mannheim, Germany). Total proteins were separated by SDS-PAGE gels and transferred onto polyvinylidene fluoride membranes (Millipore). The membranes were incubated with primary antibodies against phospho-AMPK (2535T; Cell Signaling Technology), AMPK (5831S; Cell Signaling Technology), phospho-mTOR (5536S; Cell Signaling Technology), mTOR (2983T; Cell Signaling Technology), phospho-p70S6K (Thr-389) (9205S; Cell Signaling Technology), p70S6K (9202S; Cell Signaling Technology), and β-actin (66009-1-Ig; Proteintech). Then, the membranes were incubated with species-specific HRP-conjugated secondary antibodies. ChemiDoc™ MP Imaging System (Bio-Rad, USA) was used to detect signals.

mtDNA quantification

Genomic DNA from MEFs was isolated using the DNeasy Blood and Tissue Kit (Qiagen), following the manufacturer's instructions. The mtDNA quantitative assay was repeated three times using 5 ng DNA, TaqMan Universal Master Mix II, and Life Technologies' Taq from Life Technologies. We used the CytOx2 gene as the target gene, which is a mtDNA-encoded subunit of the respiratory chain on mtDNA, to analyze mtDNA, as previously described [41]. Primers for the CytOx2 gene were: Forward, 5'-GATAACCGAGTCGTTCTGCCA-3' and Reverse, 5'-CCCTGGTCGGTTTGATGTTACT-3'. The results are expressed as the relative expression of the

CytOx2 gene normalized to the nuclear 18S gene and related to the values observed in *Ptpn11*$^{+/+}$ MEFs.

Mitochondrial stress assay

Seahorse XFe24 Analyzer (Agilent Technologies) was used to measure cellular oxygen consumption rate (OCR). In brief, MEFs were seeded (4 replicates) in XFe24 Cell Culture Microplates (#100777-004, Agilent Technologies) at approximately 90% confluency (2.5×10^4 cells/well) in DMEM supplemented with 10% FBS. Cells were cultured at 37°C until completely adherent in a humidified 5% CO_2 incubator. Before the assay, the culture medium was replaced with 500 µL of pre-prepared serum-free unbuffered Seahorse XF Base Medium (#103334-100, Agilent Technologies) at pH 7.4, which had been prewarmed to 37°C and supplemented with the agents for analysis of mitochondrial oxidative metabolism. Then, MEFs were incubated in a CO_2-free incubator at 37°C for 1 h. Cartridges equipped with oxygen- and pH-sensitive probes were preincubated with calibration solution (#100840-000, Agilent Technologies) overnight at 37°C in a CO_2-free incubator. The OCR and extracellular acidification rate (ECAR) were evaluated in a time course before and after injection of the following compounds: OCR measurement (#103015-100, Agilent Technologies): (i) 1 mM oligomycin; (ii) 0.5 mM FCCP [carbonylcyanide-4-(trifluoromethoxy)phenylhydrazone]; (iii) 0.5 mM antimycin A; ECAR measurement (#103-020-100, Agilent Technologies): (i) 10 mM glucose; (ii) 1 µM oligomycin; and (iii) 50 mM 2-deoxyglucose (2-DG). ECAR and OCR values were normalized to the total amount of protein per well. ECAR and OCR data points refer to the average rates during the measurement cycles and were reported as absolute rates (mpH/min/µg for ECAR, pmol/min/µg for OCR).

The adenosine triphosphate (ATP) production assay

For the measurement of adenosine triphosphate (ATP) levels of cells, 2×10^6 MEFs were seeded into 10-cm plates and incubated for 24 h. A total of 1×10^6 fresh cell precipitates were collected and lysed in 100 µL of ice-cold ATP assay buffer for 10 min. Next, the lysate was clarified by centrifugation (10000× g, 10 min, 4°C) and was deproteinized using a Deproteinization Sample Preparation Kit (K808, BioVision). ATP Colorimetric/Fluorometric Assay kit (#K354-100, BioVision) was used for ATP quantification. Data were normalized to the total protein quantity. The results were plotted as fold-change corrected for the control samples.

Statistical analysis

GraphPad Prism 7.0 software was used for statistical analysis. Welch t-test was used for statistical comparisons between two groups. One-way ANOVA with a Tukey's post hoc test was used for the statistical comparisons between multiple groups. *P* values lower than 0.05 indicated statistically significant differences and were classified as follows: *P<0.05, **P<0.01, ***P<0.001, P>0.05, ns (no significant differences).

Results

Arsenic increases susceptibility to Ptpn11$^{D61G/+}$*-induced malignancies*

To explore the tumorigenic effect of low-dose arsenic and the *Ptpn11*$^{D61G/+}$ mutation, we obtained MEFs from mice expressing *Ptpn11*$^{+/+}$ or *Ptpn11*$^{D61G/+}$. WT and *Ptpn11*$^{D61G/+}$-mutant MEFs were treated with different arsenic trioxide concentrations (0, 0.1, 2, and 5 µM) to simulate the effect of environmental arsenic [42]. Cell proliferation analysis revealed that 0.1 and 2 µM arsenic had a slightly toxic effect on MEFs expressing *Ptpn11*$^{+/+}$ or *Ptpn11*$^{D61G/+}$ (**Figure 1A** and **1B**), suggesting these two arsenic concentrations function like environmental carcinogens on human body. Then, we performed tumorigenesis-associated assays to examine the carcinogenic effect of arsenic on WT and mutant MEFs at different time points (*i.e.*, after 1, 2, and 3 months of arsenic exposure). We found that the introduction of *Ptpn11*$^{D61G/+}$ mutation in MEFs promoted proliferation following 3 months of arsenic treatment, compared to WT MEFs (**Figure 1C** and **1D**). Moreover, 2 µM but not 0.1 µM arsenic further promoted the proliferation of MEFs expressing *Ptpn11*$^{+/+}$ and *Ptpn11*$^{D61G/+}$ (Figure S1). To investigate whether arsenic exposure increased cell motility, we performed a transwell chamber assay to detect cell migration and invasion in arsenic-transformed MEFs following chronic 2 µM arsenic treatment. Arsenic treatment enhanced cell migration and inva-

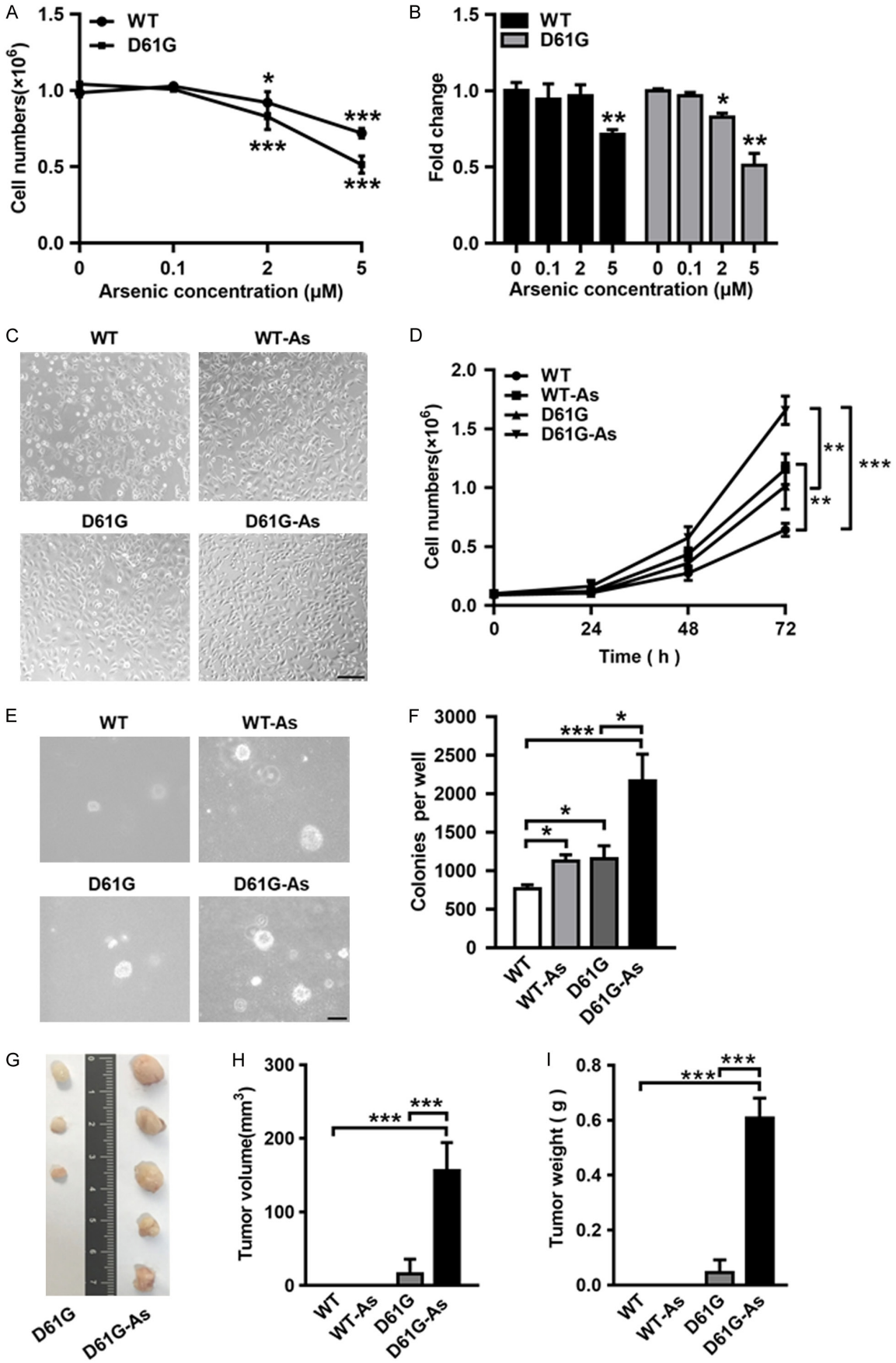
A
WT
D61G
Cell numbers(×10^6)
Arsenic concentration (μM)
B
WT
D61G
Fold change
Arsenic concentration (μM)
C
WT
WT-As
D61G
D61G-As
D
WT
WT-As
D61G
D61G-As
Cell numbers(×10^6)
Time (h)
E
WT
WT-As
D61G
D61G-As
F
Colonies per well
WT
WT-As
D61G
D61G-As
G
D61G
D61G-As
H
Tumor volume(mm^3)
WT
WT-As
D61G
D61G-As
I
Tumor weight (g)
WT
WT-As
D61G
D61G-As

Figure 1. Chronic arsenic trioxide exposure promotes malignant transformation of *Ptpn11*$^{D61G/+}$ MEFs. (A) Cell viability of WT and *Ptpn11*$^{D61G/+}$ MEFs treated with arsenic concentrations ranging from 0 to 5 μM for 72 h. (B) Cell viability was detected by MTT assay (n=3). (C) MEFs were exposed to arsenic (2 μM) for 3 months and the morphology of normal MEFs (WT, D61G) and transformed MEFs (WT-As, D61G-As) are shown. Scale bar: 40 μm. (D) The cell proliferation growth curves of four types of MEFs after 3 months of arsenic treatment. (E, F) Anchorage-independent growth in soft agar. Representative graph and number of colonies in soft agar after 3 months of treatment with 2 μM arsenic. (G-I) Arsenic-transformed *Ptpn11*$^{D61G/+}$ MEFs displayed significantly stronger tumorigenicity in nude mice. (n=5). Average tumor volumes (H), weight (I) are shown. *P<0.05, **P<0.01, ***P<0.001.

sion, especially in *Ptpn11*$^{D61G/+}$-mutant MEFs. The number of migratory and invasive cells in arsenic-treated mutant cells increased significantly compared to the untreated group (Figure S2).

We performed a soft agar assay, which revealed that mutant MEFs had enhanced anchorage-independent growth capacity compared to WT MEFs (**Figure 1E** and **1F**). Interestingly, 2 μM but not 0.1 μM arsenic increased anchorage-independent growth capacity of WT and mutant MEFs following 3-month arsenic treatment (Figure S3A and S3B), but 1- or 2-month arsenic treatment did not affect the anchorage-independent growth of WT and mutant MEFs (Figure S3C and S3D).

To examine the tumorigenic capacity of WT and mutant MEFs, we prepared MEFs *in vitro* in the presence and absence of arsenic for 3 months and performed a xenograft tumor assay. Only *Ptpn11*$^{D61G/+}$-mutant MEFs formed tumors, while the WT MEFs did not (**Figure 1G**). Additionally, arsenic treatment increased tumor weight and volume of *Ptpn11*$^{D61G/+}$-mutant MEFs tumors (**Figure 1H** and **1I**). We speculate that chronic arsenic exposure at a certain concentration can promote malignant transformation *in vitro*, but tumors to fail to form *in vivo* due to the complex factors of the mouse tumor microenvironment, including the presence of multiple immune cells. These data support the conclusion that chronic arsenic exposure can promote the malignant transformation of WT and *Ptpn11*$^{D61G/+}$-mutant MEFs.

Arsenic enhances the mitochondrial respiration of WT and Ptpn11$^{D61G/+}$*-mutant MEFs*

Continuous tumor cell proliferation requires constant energy metabolism adaptation to meet the metabolic demands of rapid cell growth and division. Mitochondrial oxidative metabolism is the primary source of cellular energy. Studies have shown that arsenic exposure may promote tumorigenesis through mitochondrial dysfunction and a metabolic switch to glycolysis [43, 44]. To determine arsenic-induced energy metabolism changes in *Ptpn11*$^{D61G/+}$-mutant cells, we used Seahorse metabolic analysis to examine metabolic alterations. We found that *Ptpn11*$^{D61G/+}$ mutation promoted mitochondrial oxidative phosphorylation (OXPHOS) at the maximum level without altering the basal level of OXPHOS (**Figure 2A**). Moreover, arsenic-treated WT MEFs showed increased oxygen consumption at basal and maximum levels compared to untreated MEFs (**Figure 2A** and **2B**). Arsenic also promoted OXPHOS in mutant MEFs (**Figure 2A-C**).

OXPHOS generates ATP and ROS by the electron transport chain. Therefore, we examined ATP production in WT and *Ptpn11*$^{D61G/+}$-mutant MEFs with or without arsenic treatment. The *Ptpn11*$^{D61G/+}$ mutation did not affect ATP production in MEFs. However, arsenic increased ATP production in WT and *Ptpn11*$^{D61G/+}$-mutant MEFs (**Figure 2D**). Additionally, we analyzed cellular ROS production by flow cytometry using DCFH-DA probe, which measures ROS levels. ROS levels in *Ptpn11*$^{D61G/+}$-mutant MEFs were higher than WT MEFs. Following arsenic treatment, WT and *Ptpn11*$^{D61G/+}$-mutant MEFs showed higher ROS production (**Figure 2E** and **2F**). These results suggest increased mitochondrial aerobic metabolism was closely associated with arsenic-induced malignant transformation.

We further tested whether arsenic causes a metabolic switch to glycolysis. There was no obvious difference in the extracellular acidification rate (ECAR) between arsenic-treated and untreated WT MEFs at the basal level, indicating that long-term low-concentration arsenic treatment had no effect on basal glycolysis levels of WT MEFs. The *Ptpn11*$^{D61G/+}$-mutated MEFs showed no obvious enhanced glycolysis compared to WT MEFs, but basal glycolysis levels in mutant cells were significantly increased following arsenic treatment (**Figure 3A** and **3B**).

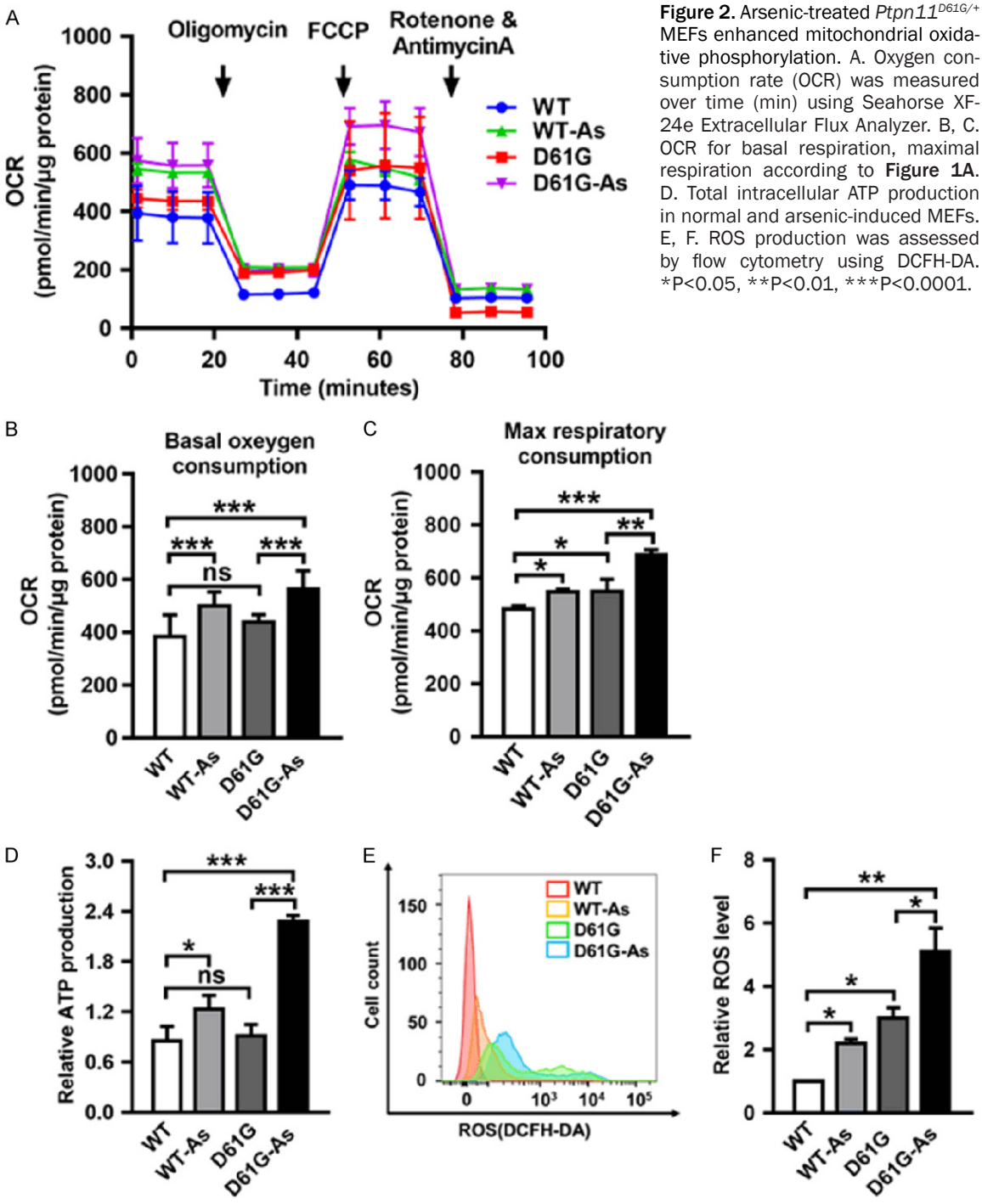

Figure 2. Arsenic-treated *Ptpn11*$^{D61G/+}$ MEFs enhanced mitochondrial oxidative phosphorylation. A. Oxygen consumption rate (OCR) was measured over time (min) using Seahorse XF-24e Extracellular Flux Analyzer. B, C. OCR for basal respiration, maximal respiration according to **Figure 1A**. D. Total intracellular ATP production in normal and arsenic-induced MEFs. E, F. ROS production was assessed by flow cytometry using DCFH-DA. *P<0.05, **P<0.01, ***P<0.0001.

As shown in **Figure 4B**, mutant cell OCR was also enhanced following arsenic treatment at the basal level. Taken together, these results indicated that both mitochondrial aerobic metabolism and glycolysis were enhanced in arsenic-treated mutant cells under normal culture conditions. To further investigate the metabolite produced during glycolysis in arsenic-induced MEFs, we measured the intracellular level of lactate, a major metabolite of the glycolysis pathway. Arsenic treatment and the *Ptpn11*$^{D61G/+}$ mutation did not affect lactate levels in MEFs (**Figure 3D**), which indicated glycolysis may not be the main energy source of arsenic-induced mutant MEFs. Because aerobic cellular metabolism is not restricted after

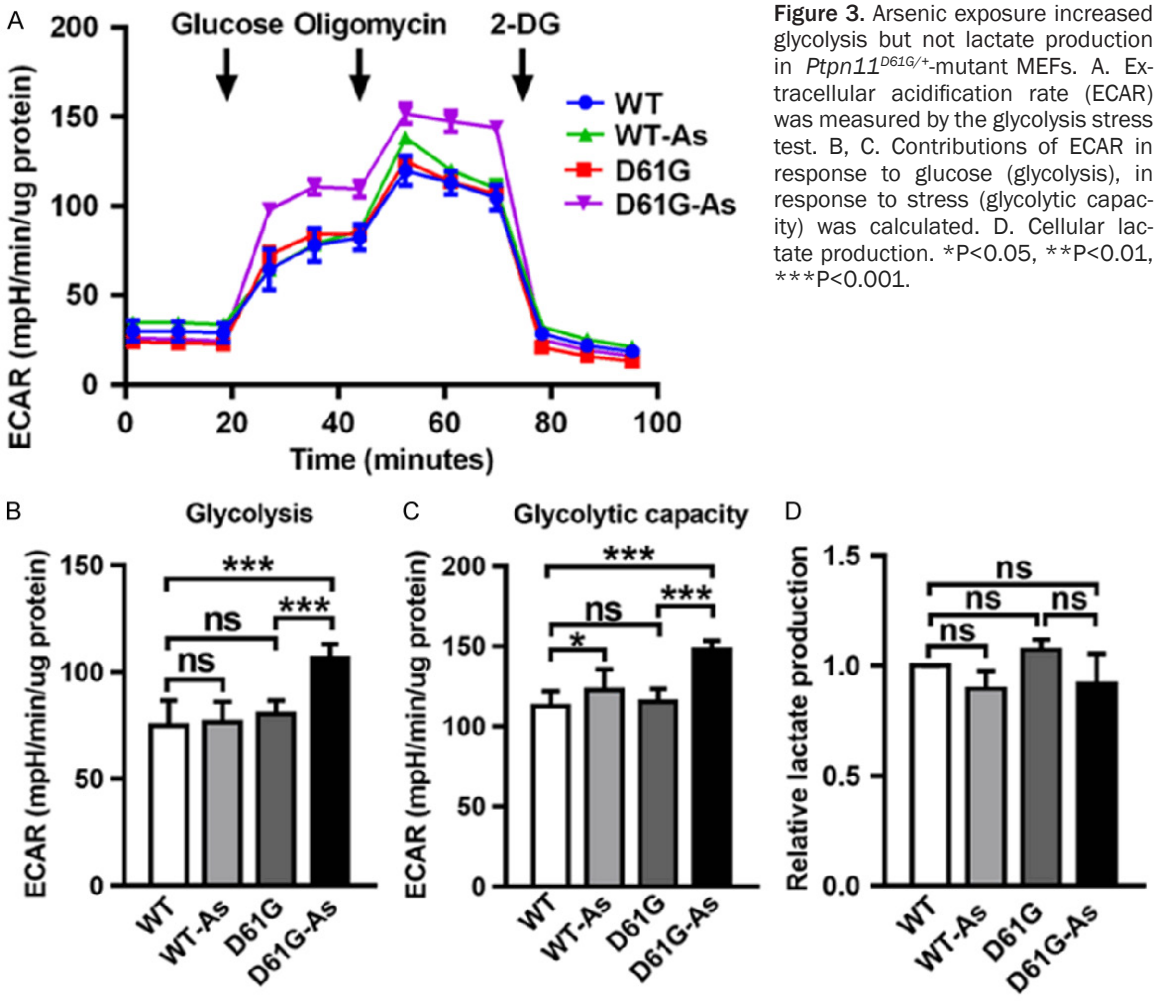

Figure 3. Arsenic exposure increased glycolysis but not lactate production in *Ptpn11*$^{D61G/+}$-mutant MEFs. A. Extracellular acidification rate (ECAR) was measured by the glycolysis stress test. B, C. Contributions of ECAR in response to glucose (glycolysis), in response to stress (glycolytic capacity) was calculated. D. Cellular lactate production. *P<0.05, **P<0.01, ***P<0.001.

glucose injection, elevated ECAR may be related to the accumulation of a large number of acid metabolites produced by aerobic metabolism, such as carbon dioxide and carbonic acid, rather than lactate. To examine the maximum glycolytic capacity, we inhibited mitochondrial aerobic metabolism with oligomycin, a drug that rapidly hyperpolarized the mitochondrial membrane by inhibiting ATP synthase to prevent protons from passing through the complex. The maximum glycolytic capacity of WT MEFs slightly increased after chronic arsenic exposure; however, the maximum glycolytic capacity of arsenic-treated *Ptpn11*$^{D61G/+}$-mutant MEFs was significantly increased compared to the untreated group (**Figure 3A** and **3C**). These data suggest arsenic-treated mutant MEFs use OXPHOS as the main energy source under basic culture conditions. Consistently, there was no significant difference in lactate production despite the increased ECAR in arsenic-treated mutant cells at the basic level. Glycolysis may serve as an alternative energy supply that cells can exploit to adapt during malignant transformation and rapid proliferation when mitochondrial oxidative metabolism is deficient or impaired.

Arsenic promoted the expression of mitochondrial complexes in both WT and Ptpn11$^{D61G/+}$*-mutant MEFs*

Given arsenic enhanced mitochondrial OXPHOS in both WT and mutant MEFs, we speculated that mitochondrial dysfunction may be the core mechanism underlying arsenic-induced malignancy. Cell electron microscopy revealed that arsenic treatment did not affect the number of mitochondria (**Figure 4A**). Consistent with these data, we measured the copy number of CytOx2, which is encoded by mitochondrial DNA, using qPCR. Data were calibrated by nuclear 18s DNA. We observed no statistically

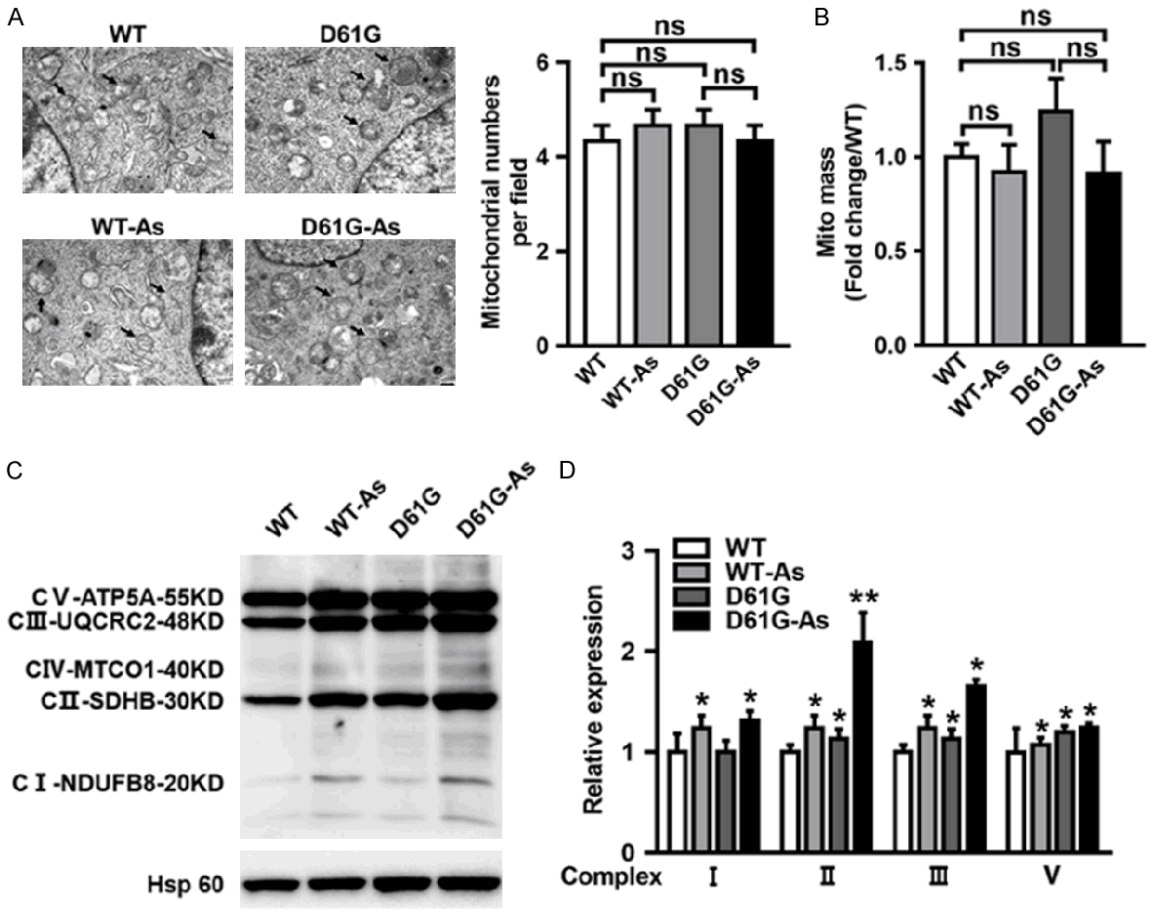

Figure 4. Mitochondrial function is increased in arsenic-treated *Ptpn11*$^{D61G/+}$-mutant MEFs. A. Representative electron microscopy pictures of mitochondria and quantification of mitochondrial number in MEFs. Scale bar: 500 nm; B. Real-time PCR amplification was used to measure relative mtDNA content. C. Increased expression of mitochondrial electron chain transport complexes in MEFs. D. Quantification of protein levels of isolated mitochondrial complex components from MEFs. *P<0.05, **P<0.01.

significant difference in the mean value of mtDNA/18s DNA ratio in the four types of MEFs mentioned (**Figure 4B**).

If the increased mitochondrial OXPHOS was not related to mitochondrial quantity, we hypothesized the increase may be caused by altered expression of electron transport chain enzymes. To that end, we examined the expression of electron transport chain complexes (SDHA for complex II, cytochrome c for complex III, COX IV for complex IV, and ATP5A for complex V). Our results revealed a slight increase in the expression of respiratory enzymes II, III, and V in mutant MEFs compared to WT MEFs, and the expression of respiratory enzymes I, II, III, and V were all increased significantly after arsenic exposure compared to the untreated group (**Figure 4C** and **4D**). Taken together, the increased expression of electron transport chain enzymes suggests they are closely associated with arsenic-induced malignancy.

Rapamycin inhibits malignant transformation of arsenic-treated Ptpn11$^{D61G/+}$*-mutant MEFs*

The molecular mechanism underlying arsenic-induced mitochondrial dysfunction remains unclear. Because mTOR signaling is the key sensor of cellular metabolism [45, 46], we examined the expression of mTOR-associated molecules. As illustrated in **Figure 5A** and **5B**, the p-mTOR/mTOR and p-P70S6K/P70S6K ratios were all increased in arsenic-induced groups, whereas the p-AMPKα/AMPKα ratio in the arsenc-induced groups was lower than that in the untreated groups, especially in the mutant MEFs. Notably, AMPK phosphorylation

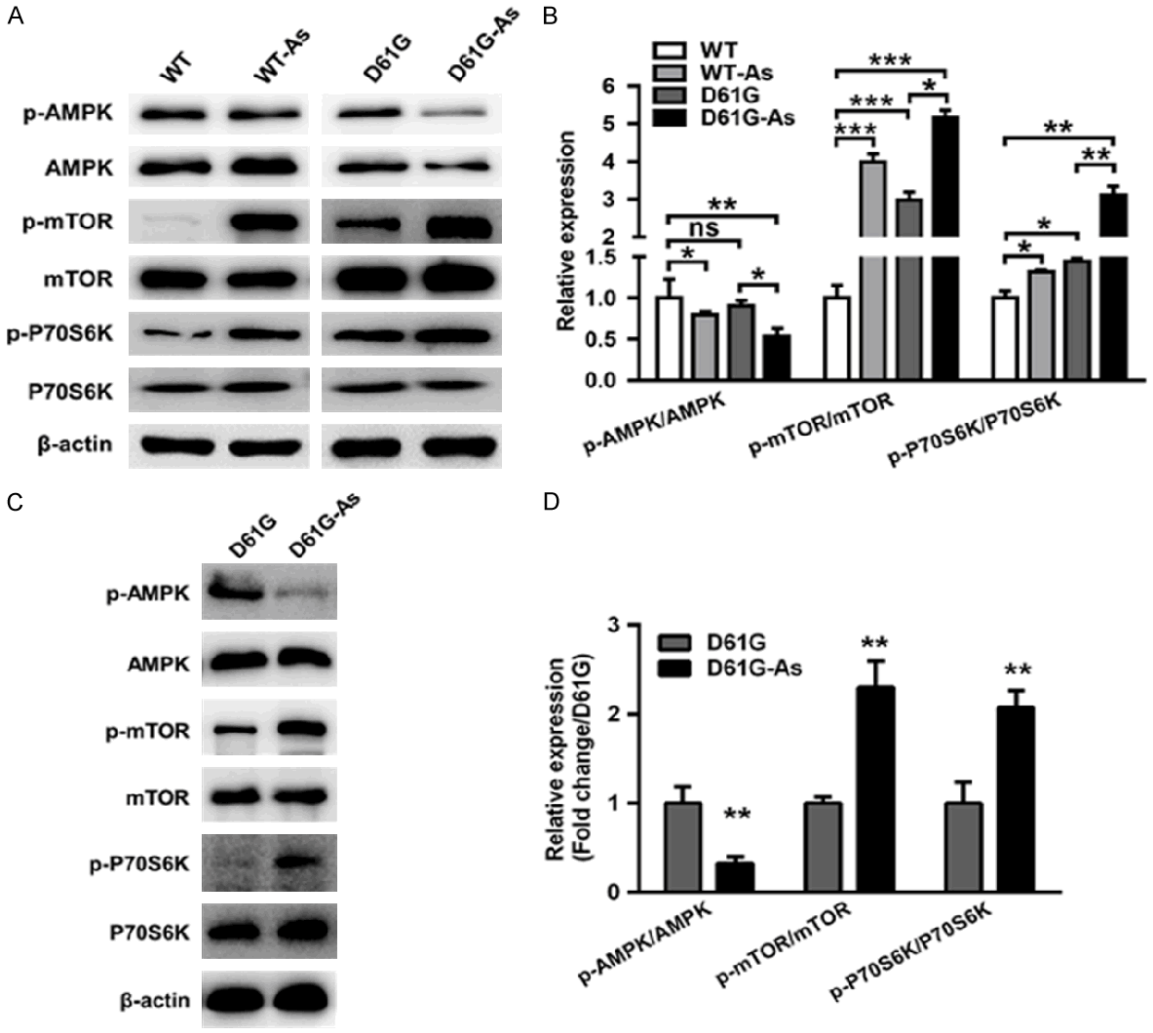

Figure 5. Arsenic-induced activation of AMPK/mTOR/P70S6K signaling pathway. The expression of AMPK/mTOR/p-P70S6K pathway members in WT and *Ptpn11*$^{D61G/+}$ MEFs (A) and tumor tissue from nude mouse xenografts (C) with or without arsenic treatment were detected by western blot. (B, D) Relative quantitative analysis of protein expression in (A and C). *P<0.05, **P<0.01, ***P<0.001.

decreased significantly after arsenic exposure. We speculated that AMPK phosphorylation levels may be related to the ratio of AMP:ATP in MEFs, which is consistent with our previous detection of elevated ATP levels in cells exposed to arsenic. Further examination of the tumor tissue from our nude mouse xenograft assay revealed a lower degree of AMPK phosphorylation and increased mTOR and p70S6K phosphorylation levels (**Figure 5C** and **5D**), suggesting AMPK/mTOR/P70S6K signaling may be involved in malignant transformation.

To further evaluate whether mTOR is important for arsenic-induced malignant transformation, we treated both WT and *Ptpn11*$^{D61G/+}$-mutant MEFs with and without rapamycin, which is the classical mTOR inhibitor. We observed a drastic reduction of mitochondrial respiration in arsenic-treated *Ptpn11*$^{D61G/+}$-mutant MEFs, compared to untreated mutant MEFs (**Figure 6A-C**). We performed a MTT assay, which revealed rapamycin treatment significantly decreased the growth of arsenic-induced WT and *Ptpn11*$^{D61G/+}$-mutant MEFs (**Figure 6D**). Additionally, we found that rapamycin treatment significantly reduced soft agar colony formation in WT and *Ptpn11*$^{D61G/+}$-mutant MEFs (**Figure 6E** and **6F**). Indeed, mTOR phosphorylation and downstream p-P70S6K decreased significantly in the arsenic-treated group compared to the untreated group (**Figure 6G**, **6H**).

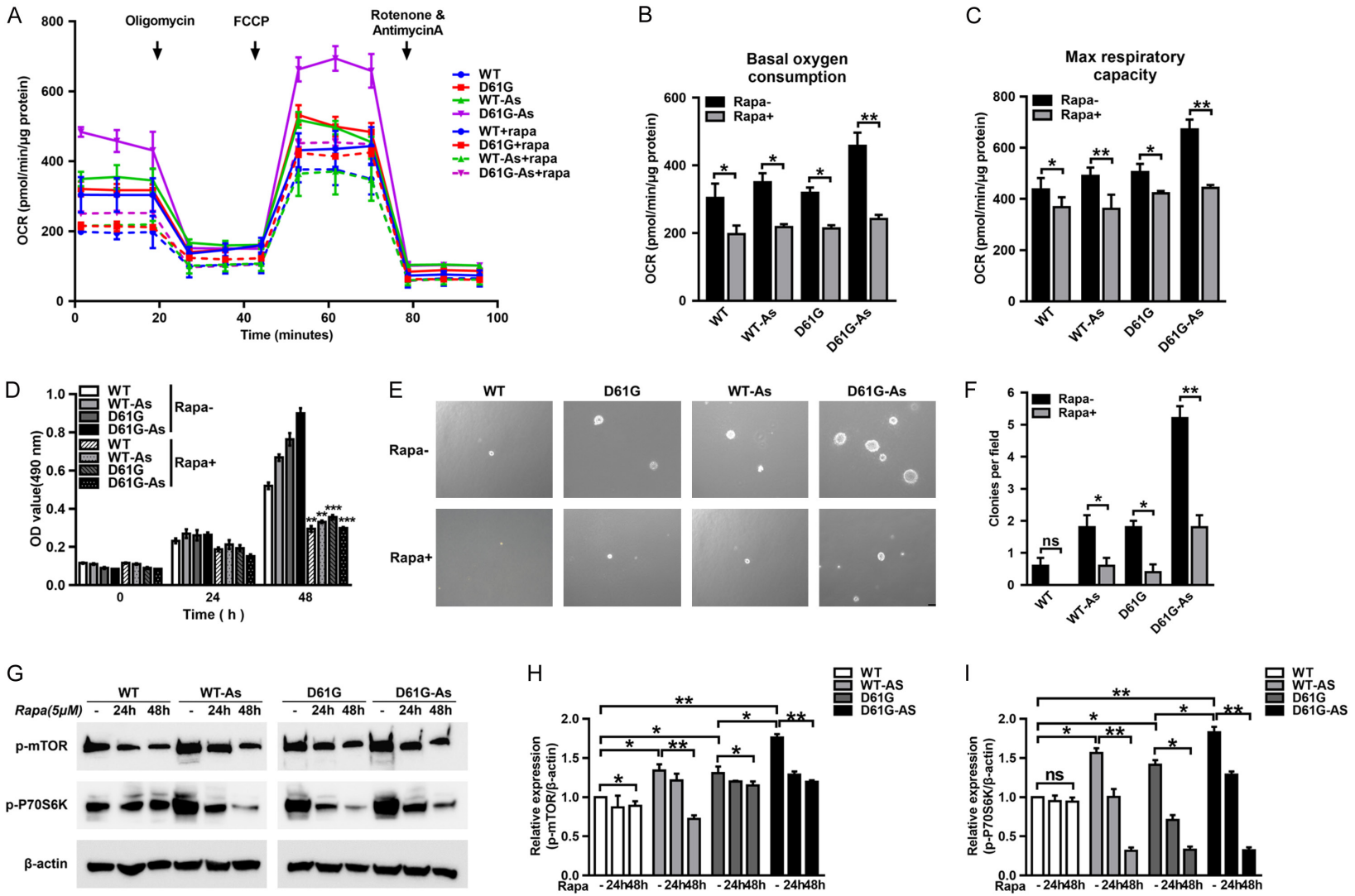

Figure 6. Rapamycin inhibits malignant transformation of *Ptpn11*$^{D61G/+}$-mutant MEFs by inhibiting mitochondrial oxidative phosphorylation. A-C. mTOR inhibitor rapamycin receded arsenic-induced OCR affluence in *Ptpn11*$^{D61G/+}$ MEFs. D. WT and *Ptpn11*$^{D61G/+}$ MEFs were treated with rapamycin for 48 h at 5 nM. Cell viability was determined by MTT assay. E, F. Soft agar experiment showed mTOR inhibitor abrogated higher anchorage-dependent growth ability in arsenic-treated *Ptpn11*$^{D61G/+}$ MEFs. G-I. WT and *Ptpn11*$^{D61G/+}$ MEFs were treated with rapamycin (5 nM) for 24 h and 48 h, and p-P70S6K and p-mTOR levels were analyzed by western blotting. *P<0.05, **P<0.01, ***P<0.001.

These results suggest arsenic promoted malignant transformation of WT and *Ptpn11*$^{D61G/+}$-mutant MEFs through activation of the mTOR signaling pathway.

Discussion

Low-dose arsenic exposure can cause malignant tumors. Because arsenic-induced tumors are often multiorgan tumors, there is no widely accepted arsenic tumor-inducing model for research. Moreover, due to population genetic polymorphisms, low-dose arsenic exposure may produce discrepant carcinogenic results. Therefore, the superposition of environmental pollution and genetic polymorphisms makes certain populations more susceptible to tumor development. Because the *Ptpn11*$^{D61G/+}$ mutation only increases the small magnitude of phosphatase activity, it is a relatively weak tumor-causing gene mutation. Therefore, we explored whether a weakly oncogenic mutation and arsenic exposure can synergistically promote tumor development and progression. Our results demonstrate that chronic low-concentration arsenic treatment increased the malignant transformation ability of *Ptpn11*$^{D61G/+}$-mutated MEFs. Functionally, low arsenic concentrations promoted malignant transformation of MEFs by increasing the oxidative respiration capacity of *Ptpn11*$^{D61G/+}$-mutant cells, thereby increasing cell energy metabolism. Interestingly, low concentrations of arsenic did not have a significant effect on WT MEFs energy metabolism, which demonstrates that arsenic induction increases the cancer susceptibility associated with gene mutations. However, whether the mechanism is due to the superimposed effect of the two or arsenic-induced enhancement of the phosphorylation ability of *Ptpn11*$^{D61G/+}$ remains unknown.

Previously, the well-known Warburg effect posited that tumor cells are more dependent on glycolysis for energy than the tricarboxylic acid cycle. It is generally believed that glycolysis can produce energy more quickly and produce a large number of intermediate products that participate in other cellular metabolic pathways that facilitate rapid tumor cell division and proliferation. However, the tricarboxylic acid cycle is actually increased in cancer stem cells, especially leukemia stem cells. Also, we showed that arsenic increased aerobic respiration MEFs, which also show stemness, to enhance their malignant transformation. This finding indicates that enhanced aerobic respiration is also necessary for tumor development. Critically, arsenic promotes this ability by increasing mTOR signaling. As the sensor of cellular energy metabolism, mTOR is highly conserved in biological evolution and plays an important role in proliferation, metabolism, autophagy, and apoptosis [45].

Pervious research has demonstrated that ROS, energy synthesis, hypoxia stimulation, and amino acids are involved in tumor initiation and progression through mTOR signaling pathway [47]. ROS-induced oxidative stress, which is produced during arsenic methylation, is the main mechanism of arsenic carcinogenesis [48]. In our study, we demonstrated that ROS levels and ATP production were increased in MEFs after chronic arsenic treatment. Chronic arsenic treatment can stimulate mTOR activation, which is consistent with our results that arsenic treatment enhanced mTOR and downstream P70S6K phosphorylation. Moreover, the GOF mutant Ptpn11 can also activate the mTOR signaling pathway. Furthermore, mTOR inhibitor rapamycin markedly reduced mitochondrial hypermetabolism and cell proliferation induced by arsenic exposure. Therefore, it appears mTOR signaling may be a key pathway that mediates the synergistic carcinogenesis between the *Ptpn11*$^{D61G/+}$ mutation and chronic arsenic exposure.

In summary, our research shows that arsenic exposure further enhances the activation of mTOR signaling to enhance aerobic respiratory function. Critically, inhibiting mTOR signaling significantly inhibits the carcinogenic effects induced by arsenic exposure and the Ptpn11 mutation. The excessive mTOR activation caused by the *Ptpn11*$^{D61G/+}$ mutation increases aerobic respiration. Therefore, targeting this mTOR-mitochondrial metabolism axis may represent a cancer prevention or therapeutic target to reduce the cancer burden in arsenic-exposed individuals with Ptpn11 mutation.

Acknowledgements

This work was supported by the National Natural Science Foundation of China (81472-087); and the Natural Science Research program for Anhui Higher Education Institutions (KJ2020A0192).

Disclosure of conflict of interest

None.

Address correspondence to: Siying Wang, Department of Pathophysiology, School of Basic Medical Sciences, Anhui Medical University, Hefei 230032, Anhui, China. E-mail: sywang@ahmu.edu.cn

References

[1] Huang KL, Mashl RJ, Wu Y, Ritter DI, Wang J, Oh C, Paczkowska M, Reynolds S, Wyczalkowski MA, Oak N, Scott AD, Krassowski M, Cherniack AD, Houlahan KE, Jayasinghe R, Wang LB, Zhou DC, Liu D, Cao S, Kim YW, Koire A, McMichael JF, Hucthagowder V, Kim TB, Hahn A, Wang C, McLellan MD, Al-Mulla F, Johnson KJ; Cancer Genome Atlas Research Network, Lichtarge O, Boutros PC, Raphael B, Lazar AJ, Zhang W, Wendl MC, Govindan R, Jain S, Wheeler D, Kulkarni S, Dipersio JF, Reimand J, Meric-Bernstam F, Chen K, Shmulevich I, Plon SE, Chen F and Ding L. Pathogenic germline variants in 10,389 adult cancers. Cell 2018; 173: 355-370.

[2] Ginsburg O, Ashton-Prolla P, Cantor A, Mariosa D and Brennan P. The role of genomics in global cancer prevention. Nat Rev Clin Oncol 2021; 18: 116-128.

[3] Arita A and Costa M. Epigenetics in metal carcinogenesis: nickel, arsenic, chromium and cadmium. Metallomics 2009; 1: 222-228.

[4] Chen QY, DesMarais T and Costa M. Metals and mechanisms of carcinogenesis. Annu Rev Pharmacol Toxicol 2019; 59: 537-554.

[5] Mittelstrass K, Sauter W, Rosenberger A, Illig T, Timofeeva M, Klopp N, Dienemann H, Meese E, Sybrecht G, Woelke G, Cebulla M, Degen M, Morr H, Drings P, Groeschel A, Kreymborg KG, Haeussinger K, Hoeffken G, Schmidt C, Jilge B, Schmidt W, Ko YD, Taeuscher D, Chang-Claude J, Wichmann HE, Bickeboeller H and Risch A. Early onset lung cancer, cigarette smoking and the SNP309 of the murine double minute-2 (MDM2) gene. BMC Cancer 2008; 8: 113.

[6] Stoffel EM and Murphy CC. Epidemiology and mechanisms of the increasing incidence of colon and rectal cancers in young adults. Gastroenterology 2020; 158: 341-353.

[7] Chan RJ and Feng GS. PTPN11 is the first identified proto-oncogene that encodes a tyrosine phosphatase. Blood 2007; 109: 862-867.

[8] Mohi MG and Neel BG. The role of Shp2 (PTPN11) in cancer. Curr Opin Genet Dev 2007; 17: 23-30.

[9] Feng GS, Shen R, Heng HH, Tsui LC, Kazlauskas A and Pawson T. Receptor-binding, tyrosine phosphorylation and chromosome localization of the mouse SH2-containing phosphotyrosine phosphatase Syp. Oncogene 1994; 9: 1545-1550.

[10] Hof P, Pluskey S, Dhe-Paganon S, Eck MJ and Shoelson SE. Crystal structure of the tyrosine phosphatase SHP-2. Cell 1998; 92: 441-450.

[11] Lu W, Gong D, Bar-Sagi D and Cole PA. Site-specific incorporation of a phosphotyrosine mimetic reveals a role for tyrosine phosphorylation of SHP-2 in cell signaling. Mol Cell 2001; 8: 759-769.

[12] Bentires-Alj M, Paez JG, David FS, Keilhack H, Halmos B, Naoki K, Maris JM, Richardson A, Bardelli A, Sugarbaker DJ, Richards WG, Du J, Girard L, Minna JD, Loh ML, Fisher DE, Velculescu VE, Vogelstein B, Meyerson M, Sellers WR and Neel BG. Activating mutations of the noonan syndrome-associated SHP2/PTPN11 gene in human solid tumors and adult acute myelogenous leukemia. Cancer Res 2004; 64: 8816-8820.

[13] Tartaglia M, Mehler EL, Goldberg R, Zampino G, Brunner HG, Kremer H, van der Burgt I, Crosby AH, Ion A, Jeffery S, Kalidas K, Patton MA, Kucherlapati RS and Gelb BD. Mutations in PTPN11, encoding the protein tyrosine phosphatase SHP-2, cause Noonan syndrome. Nat Genet 2001; 29: 465-468.

[14] Xu D, Wang S, Yu WM, Chan G, Araki T, Bunting KD, Neel BG and Qu CK. A germline gain-of-function mutation in Ptpn11 (Shp-2) phosphatase induces myeloproliferative disease by aberrant activation of hematopoietic stem cells. Blood 2010; 116: 3611-3621.

[15] Araki T, Mohi MG, Ismat FA, Bronson RT, Williams IR, Kutok JL, Yang W, Pao LI, Gilliland DG, Epstein JA and Neel BG. Mouse model of Noonan syndrome reveals cell type- and gene dosage-dependent effects of Ptpn11 mutation. Nat Med 2004; 10: 849-857.

[16] Zhao Y, Lin L, Zhang Y and Geng D. SHP-2 activating mutation promotes malignant biological behaviors of glioma cells. Med Sci Monit 2017; 23: 2931-2938.

[17] Hu Z, Wang X, Fang H, Liu Y, Chen D, Zhang Q, Liu X, Wei D, Qu C and Wang S. A tyrosine phosphatase SHP2 gain-of-function mutation enhances malignancy of breast carcinoma. Oncotarget 2016; 7: 5664-5676.

[18] Chan RJ, Leedy MB, Munugalavadla V, Voorhorst CS, Li Y, Yu M and Kapur R. Human somatic PTPN11 mutations induce hematopoietic-cell hypersensitivity to granulocyte-macrophage colony-stimulating factor. Blood 2005; 105: 3737-3742.

[19] Martinez VD, Vucic EA, Becker-Santos DD, Gil L and Lam WL. Arsenic exposure and the induction of human cancers. J Toxicol 2011; 2011: 431287.

[20] Monteiro De Oliveira EC, Caixeta ES, Santos VSV and Pereira BB. Arsenic exposure from groundwater: environmental contamination, human health effects, and sustainable solutions. J Toxicol Environ Health B Crit Rev 2021; 24: 119-135.
[21] Chen Y, Parvez F, Gamble M, Islam T, Ahmed A, Argos M, Graziano JH and Ahsan H. Arsenic exposure at low-to-moderate levels and skin lesions, arsenic metabolism, neurological functions, and biomarkers for respiratory and cardiovascular diseases: review of recent findings from the Health Effects of Arsenic Longitudinal Study (HEALS) in Bangladesh. Toxicol Appl Pharmacol 2009; 239: 184-192.
[22] Young JL, Cai L and States JC. Impact of prenatal arsenic exposure on chronic adult diseases. Syst Biol Reprod Med 2018; 64: 469-483.
[23] Tam LM, Price NE and Wang Y. Molecular mechanisms of arsenic-induced disruption of DNA repair. Chem Res Toxicol 2020; 33: 709-726.
[24] Chen Y, Graziano JH, Parvez F, Hussain I, Momotaj H, van Geen A, Howe GR and Ahsan H. Modification of risk of arsenic-induced skin lesions by sunlight exposure, smoking, and occupational exposures in Bangladesh. Epidemiology 2006; 17: 459-467.
[25] Wang Z, Yang P, Xie J, Lin HP, Kumagai K, Harkema J and Yang C. Arsenic and benzo[a]pyrene co-exposure acts synergistically in inducing cancer stem cell-like property and tumorigenesis by epigenetically down-regulating SOCS3 expression. Environ Int 2020; 137: 105560.
[26] Li L, Bi Z, Wadgaonkar P, Lu Y, Zhang Q, Fu Y, Thakur C, Wang L and Chen F. Metabolic and epigenetic reprogramming in the arsenic-induced cancer stem cells. Semin Cancer Biol 2019; 57: 10-18.
[27] Ruan Y, Fang X, Guo T, Liu Y, Hu Y, Wang X, Hu Y, Gao L, Li Y, Pi J and Xu Y. Metabolic reprogramming in the arsenic carcinogenesis. Ecotoxicol Environ Saf 2022; 229: 113098.
[28] Pavlova NN and Thompson CB. The emerging hallmarks of cancer metabolism. Cell Metab 2016; 23: 27-47.
[29] Liu R, Li Y, Tian L, Shi H, Wang J, Liang Y, Sun B, Wang S, Zhou M, Wu L, Nie J, Lin B, Tang S, Zhang Y, Wang G, Zhang C, Han J, Xu B, Liu L, Gong K and Zheng T. Gankyrin drives metabolic reprogramming to promote tumorigenesis, metastasis and drug resistance through activating beta-catenin/c-Myc signaling in human hepatocellular carcinoma. Cancer Lett 2019; 443: 34-46.
[30] Boroughs LK and DeBerardinis RJ. Metabolic pathways promoting cancer cell survival and growth. Nat Cell Biol 2015; 17: 351-359.
[31] Li Z and Zhang H. Reprogramming of glucose, fatty acid and amino acid metabolism for cancer progression. Cell Mol Life Sci 2016; 73: 377-392.
[32] Wallace DC. Mitochondria and cancer. Nat Rev Cancer 2012; 12: 685-698.
[33] Weinhouse S. On respiratory impairment in cancer cells. Science 1956; 124: 267-269.
[34] Farge T, Saland E, de Toni F, Aroua N, Hosseini M, Perry R, Bosc C, Sugita M, Stuani L, Fraisse M, Scotland S, Larrue C, Boutzen H, Feliu V, Nicolau-Travers ML, Cassant-Sourdy S, Broin N, David M, Serhan N, Sarry A, Tavitian S, Kaoma T, Vallar L, Iacovoni J, Linares LK, Montersino C, Castellano R, Griessinger E, Collette Y, Duchamp O, Barreira Y, Hirsch P, Palama T, Gales L, Delhommeau F, Garmy-Susini BH, Portais JC, Vergez F, Selak M, Danet-Desnoyers G, Carroll M, Recher C and Sarry JE. Chemotherapy-resistant human acute myeloid leukemia cells are not enriched for leukemic stem cells but require oxidative metabolism. Cancer Discov 2017; 7: 716-735.
[35] Ashton TM, McKenna WG, Kunz-Schughart LA and Higgins GS. Oxidative phosphorylation as an emerging target in cancer therapy. Clin Cancer Res 2018; 24: 2482-2490.
[36] Lowman XH, Hanse EA, Yang Y, Ishak Gabra MB, Tran TQ, Li H and Kong M. p53 promotes cancer cell adaptation to glutamine deprivation by upregulating Slc7a3 to increase arginine uptake. Cell Rep 2019; 26: 3051-3060.
[37] Walenta S, Wetterling M, Lehrke M, Schwickert G, Sundfor K, Rofstad EK and Mueller-Klieser W. High lactate levels predict likelihood of metastases, tumor recurrence, and restricted patient survival in human cervical cancers. Cancer Res 2000; 60: 916-921.
[38] Netea-Maier RT, Smit JWA and Netea MG. Metabolic changes in tumor cells and tumor-associated macrophages: a mutual relationship. Cancer Lett 2018; 413: 102-109.
[39] Howerton K, Schlaepfer DD and Ilic D. Establishment of cell lines from mouse embryos with early embryonic lethality. Cell Commun Adhes 2008; 15: 379-383.
[40] Sun Q, Yu X, Peng C, Liu N, Chen W, Xu H, Wei H, Fang K, Dong Z, Fu C, Xu Y and Lu W. Activation of SREBP-1c alters lipogenesis and promotes tumor growth and metastasis in gastric cancer. Biomed Pharmacother 2020; 128: 110274.
[41] Viengchareun S, Caron M, Auclair M, Kim MJ, Frachon P, Capeau J, Lombes M and Lombes A. Mitochondrial toxicity of indinavir, stavudine and zidovudine involves multiple cellular targets in white and brown adipocytes. Antivir Ther 2007; 12: 919-929.

[42] Argos M, Ahsan H and Graziano JH. Arsenic and human health: epidemiologic progress and public health implications. Rev Environ Health 2012; 27: 191-195.
[43] Yen YP, Tsai KS, Chen YW, Huang CF, Yang RS and Liu SH. Arsenic induces apoptosis in myoblasts through a reactive oxygen species-induced endoplasmic reticulum stress and mitochondrial dysfunction pathway. Arch Toxicol 2012; 86: 923-933.
[44] Luo F, Zou Z, Liu X, Ling M, Wang Q, Wang Q, Lu L, Shi L, Liu Y, Liu Q and Zhang A. Enhanced glycolysis, regulated by HIF-1alpha via MCT-4, promotes inflammation in arsenite-induced carcinogenesis. Carcinogenesis 2017; 38: 615-626.
[45] Yang X, Yang C, Farberman A, Rideout TC, de Lange CF, France J and Fan MZ. The mammalian target of rapamycin-signaling pathway in regulating metabolism and growth. J Anim Sci 2008; 86: E36-50.
[46] Cunningham JT, Rodgers JT, Arlow DH, Vazquez F, Mootha VK and Puigserver P. mTOR controls mitochondrial oxidative function through a YY1-PGC-1alpha transcriptional complex. Nature 2007; 450: 736-740.
[47] Hua H, Kong Q, Zhang H, Wang J, Luo T and Jiang Y. Targeting mTOR for cancer therapy. J Hematol Oncol 2019; 12: 71.
[48] Bach J, Peremarti J, Annangi B, Marcos R and Hernandez A. Oxidative DNA damage enhances the carcinogenic potential of in vitro chronic arsenic exposures. Arch Toxicol 2016; 90: 1893-1905.

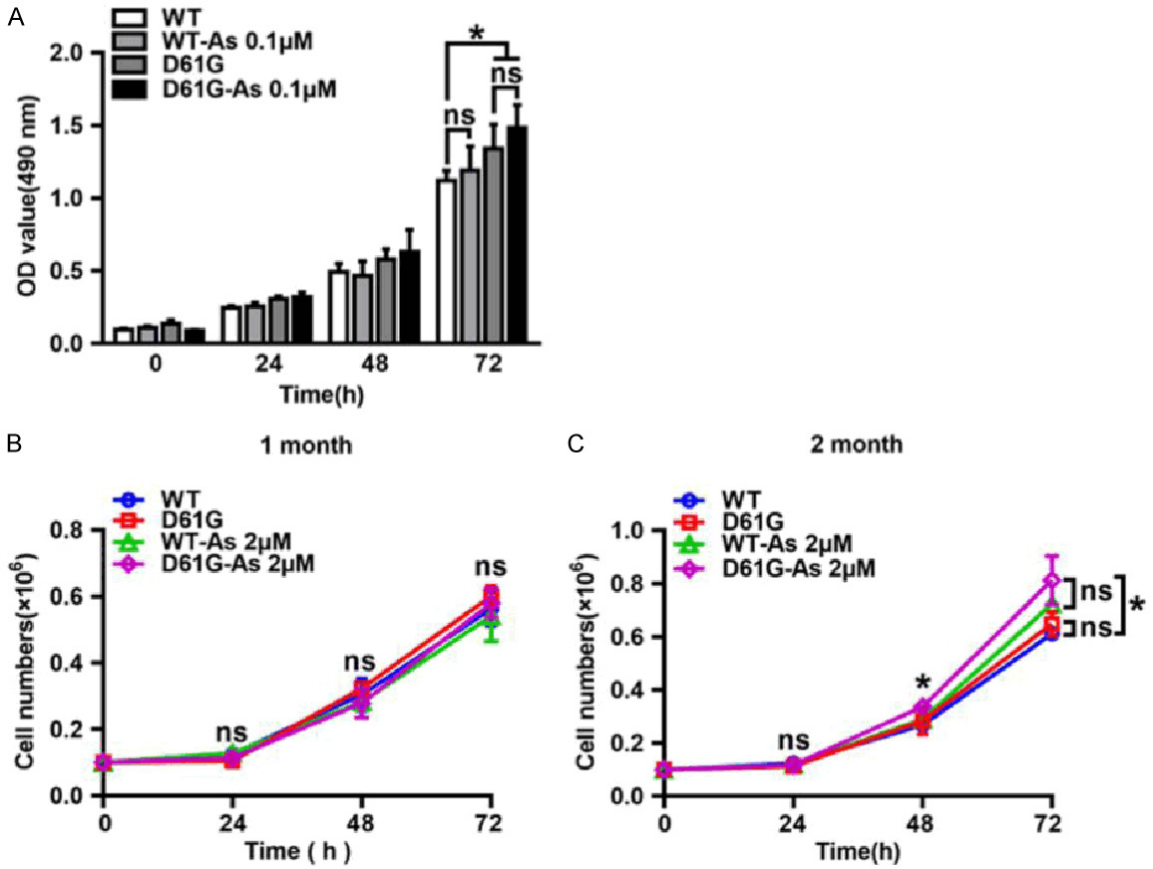

Figure S1. Effects of low concentrations of arsenic exposure on proliferation of WT and *Ptpn11*$^{D61G/+}$ MEFs. A. WT and *Ptpn11*$^{D61G/+}$ MEFs were treated with 0.1 μM arsenic for 3 months. MTT assay was performed to estimate cell proliferation every 24 h up to 72 h. B, C. Cell proliferation curves of 2 μM chronic arsenic-treated MEFs at 1 and 2 months. Data are presented as mean ± SD of triplicate experiments. *P<0.05; **P<0.01; ns, no statistical significance.

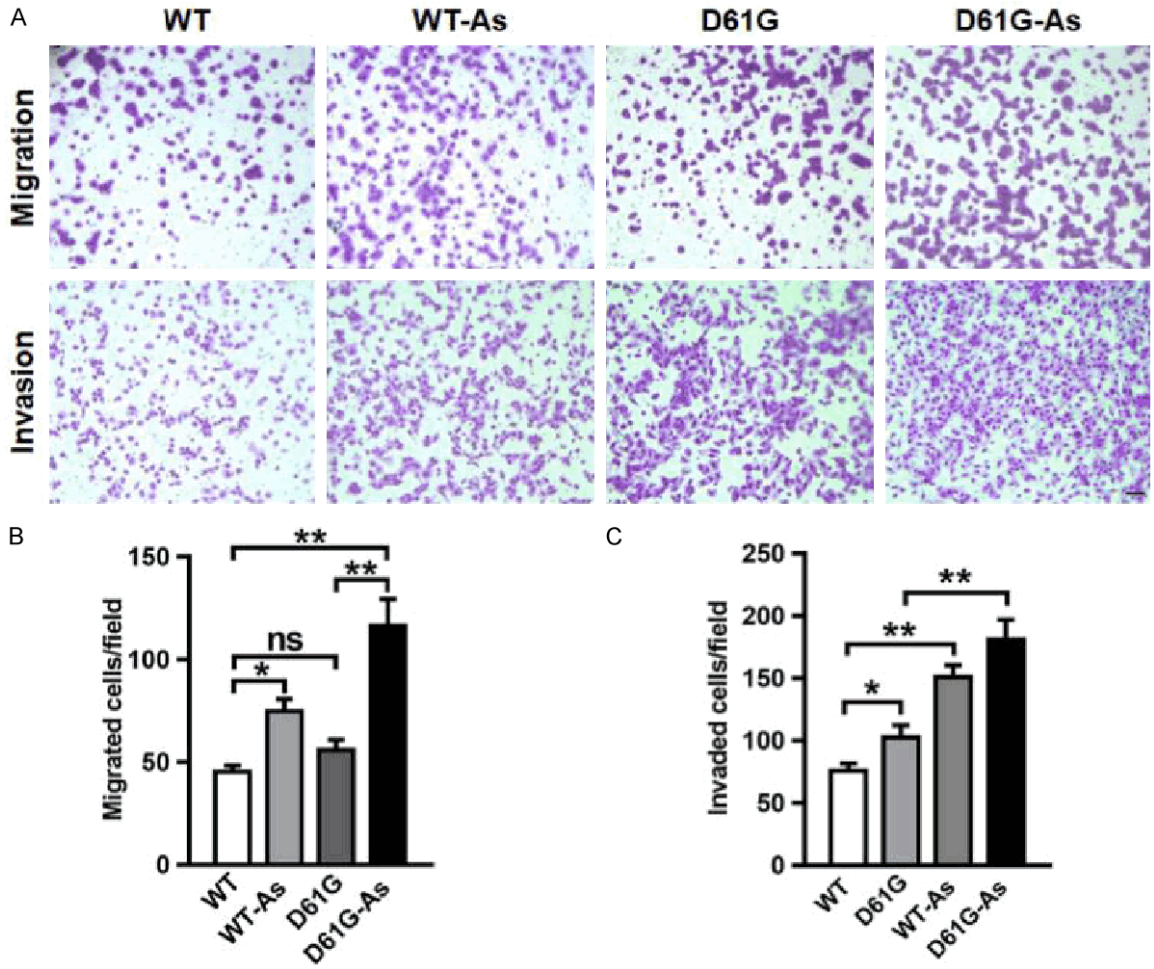

Figure S2. Chronic arsenic treatment promotes migration and invasion in *Ptpn11*$^{D61G/+}$-mutant MEFs. A. Representative images of transwell cell migration (top) and invasion (bottom) assays, photos were taken at 200× magnification. B, C. Quantitative analysis of migration and invasion capacity, the number of migratory and invasive cells in each field was calculated. Data are presented as mean ± SD of triplicate experiments. *P<0.05; **P<0.01; ns, no statistical significance.

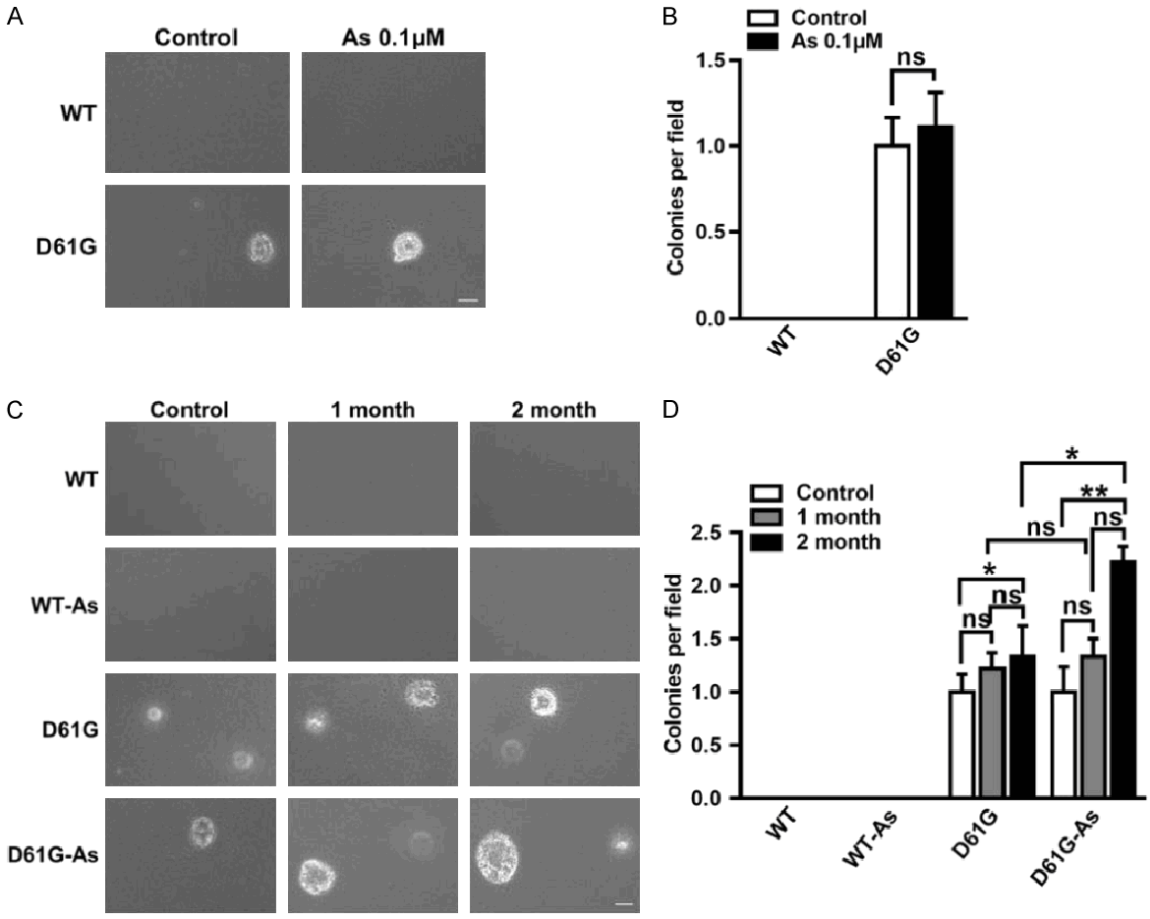

Figure S3. Effects of low concentrations of arsenic exposure on malignant transformation of WT and *Ptpn11*$^{D61G/+}$-mutant MEFs. A, B. Representative images and number of colonies in soft agar after 5 months of vehicle control treatment (phosphate buffer saline) and 0.1 μM arsenic of WT and *Ptpn11*$^{D61G/+}$ MEFs. C, D. Images and number of colonies in soft agar after 1 month and 2 months of vehicle control treatment (phosphate buffer saline) and 2 μM arsenic of WT and *Ptpn11*$^{D61G/+}$ MEFs. The results are shown as the mean ± S.D. of three independent experiments. *P<0.05; **P<0.01; ns, no statistical significance. Soft agar photos were taken at 200× magnifications.